Physics Letters A 375 (2011) 689–697

Contents lists available at ScienceDirect

Physics Letters A

www.elsevier.com/locate/pla

Inverse freezing in the Hopfield fermionic Ising spin glass with a transverse magnetic field

C.V. Morais [a], F.M. Zimmer [a], S.G. Magalhaes [b,*]

[a] Departamento de Fisica, Universidade Federal de Santa Maria, 97105-900 Santa Maria, RS, Brazil
[b] Instituto de Fisica, Universidade Federal Fluminense, 24210-346 Niterói, RJ, Brazil

ARTICLE INFO

Article history:
Received 23 August 2010
Received in revised form 28 October 2010
Accepted 6 December 2010
Available online 7 December 2010
Communicated by A.R. Bishop

Keywords:
Quantum spin glass
Fermionic model
Inverse freezing transition

ABSTRACT

The Hopfield fermionic Ising spin glass (HFISG) model in the presence of a magnetic transverse field Γ is used to study the inverse freezing transition. The mean field solution of this model allows introducing a parameter a that controls the frustration level. Particularly, in the present fermionic formalism, the chemical potential μ and the Γ provide a magnetic dilution and quantum spin flip mechanism, respectively. Within the one step replica symmetry solution and the static approximation, the results show that the reentrant transition between the spin glass and the paramagnetic phases, which is related to the inverse freezing for a certain range of μ, is gradually suppressed when the level of frustration a is decreased. Nevertheless, the quantum fluctuations caused by Γ can destroy this inverse freezing for any value of a.

1. Introduction

Recently, a kind of phase transitions called inverse transitions (melting or freezing) has attracted special interest. In this kind of transitions the ordered phase has higher entropy than the disordered one [1]. Although utterly counter-intuitive, such transitions can be found in distinct physical systems such as polymers [2], magnetic thin films [3] and high temperatures superconductors [4]. From the theoretical side, several models have been studied (mostly of them magnetic) in order to establish which mechanisms could be responsible for the existence of inverse transitions [5–13]. However, none of these mechanisms have been rigorously identified and as a consequence, they still remain to be specified [14].

An advantage of the magnetic models is that these mechanisms could be more easily identified. For instance, in the Blume–Capel (BC) model [15], it is strictly necessary to impose an extra degeneracy of the interacting states to produce an inverse melting [5]. In this particular case, inverse melting means that there is a phase transition from paramagnetism (PM) to ferromagnetism when the temperature is increased. By contrast, in the disordered counterpart of the BC model, the Ghatak–Sherrington (GS) model [16], the inverse freezing appears naturally [5,6]. To put it more precisely, in the GS model there is an inverse freezing first order phase transition from PM to spin glass (SG) when the temperature is increased. However, this transition occurs without any extra degeneracy of the interacting states as it has been done in the BC model [6].

The comparison between the BC and the GS models gives some hints on which conditions are needed in a certain model to present inverse transitions. Firstly, it should be remarked that the common feature of BC and the GS models is the existence of energetic favouring of the non-interacting spins states $S = 0$ as compared to the interacting ones $S = \pm 1$ [5]. That is provided by the anisotropic term in the Hamiltonian. In other words, there is a mechanism which favor the dilution in the BC and GS models. Nevertheless, dilution is not enough to explain the existence of inverse transitions. The question, in fact, is why in the GS model the inverse freezing appears naturally while in the BC model there is no inverse melting, unless by using a rather artificial procedure. This consideration indicates that the simultaneous presence of dilution and the non-trivial disorder known as frustration [17] is the necessary condition to obtain naturally inverse freezing. In order to check the previous suggestion, it would be needed a model in which it would be possible to control not only the level of dilution but also of frustration.

The purpose of the present work is to study the Hopfield fermionic Ising spin glass (HFISG) model in the presence of a transverse field Γ. This model belongs to a class of disordered magnetic models proposed to study the SG problem in which the spins are given as

* Corresponding author.
E-mail address: sgmagal@gmail.com (S.G. Magalhaes).

0375-9601/
doi:10.1016/j.physleta.2010.12.001

bilinear combinations of creation and destruction fermionic operators [18,19,11]. In that case, there are four possible eigenvalues of the operator S_i^z, two of them non-magnetic. In this context, the dilution means favoring of the non-magnetic states (double occupation or empty sites). The great advantage of such formulation is that it allows to investigate the combined effect of charge and spin fluctuations provided by the chemical potential μ and the transverse magnetic field Γ, respectively. In the particular case of the HFISG model, there is other important additional advantage. In its mean field solution, a parameter can be introduced to adjust the level of frustration in the problem [20]. In fact, the HFISG has been recently studied [11]. In the strong frustration limit, T_f has a reentrance which is associated to the inverse freezing as the GS model. However, when the level of frustration is decreased, the reentrance is increasingly suppressed. In particular, the SG phase is replaced by the so-called Mattis state which presents a thermodynamics similar to the usual ferromagnetism [20]. Therefore, the HFISG model with $\Gamma = 0$ is certainly a good starting point. It not only presents inverse freezing but also allows studying how the inverse freezing is affected when the level of frustration is varied.

The role of Γ in the problem deserves special attention. For instance, its effect has been extensively studied in the so-called fermionic Ising spin glass (FISG) model [18,19]. This model presents naturally inverse freezing for a certain range of μ similar to the HFISG model [10]. In the FISG, the random spin coupling J_{ij} is given as the Sherrington–Kirkpatrick model [21] which corresponds to the strong frustration limit of the HFISG model [22]. Nevertheless, if Γ is turned on, the inverse transition can be suppressed [10]. Such surprisingly effect seems to be related to the average occupation of fermions by site n. When Γ enhances, the freezing temperature T_f is depressed [23]. As consequence, the occupation of non-magnetic states near T_f becomes increasingly unimportant which is reflected on the behavior of n [24]. It tends to remain at half-filling even when μ is increased [25]. Therefore, one can speculate that the simultaneous adjusting of Γ and the level of frustration in the HFISG model would allow, for a given level of frustration, inducing a charge redistribution by the increase of Γ which would lead to suppress the inverse freezing itself. As that procedure could be done from the weak frustration to the strong frustration limit, one could probe the role of these elements, frustration and dilution as necessary conditions responsible to produce inverse freezing.

The present problem is formulated within integral functional formalism where the spins are written as bilinear combinations of Grassmann fields. The grand canonical potential is obtained using the replica method and the static approximation (SA) [26]. The SA in the present problem is justified since small values of Γ which are far from the quantum critical point Γ_c [25], are used. In particular, the SG order parameter is treated within the replica symmetry (RS) and one-step replica symmetry breaking (1S-RSB) schemes [27]. The procedure used in the present work is similar to that one used in Ref. [11]. The grand canonical potential is calculated at a mean field level in which a parameter which allows changing the level of frustration is introduced. Therefore, solutions for the saddle point order parameters can be found at different levels of frustration and Γ. The location of the first order SG/PM boundary phase is done in the present work using the criteria proposed in Ref. [28] for the GS model. It means that the chosen SG solution in the transition is that one which meets continuously the SG solution at small μ. In this case, the 1S-RSB approximation improves the SG grand canonical potential and consequently, the location of the SG first-order transitions.

Finally, it should be remarked that in this formulation, there are two versions of HFISG model. In the first one (4S model), both magnetic and non-magnetic states are allowed. In the second one (2S model), a restriction that eliminates the non-magnetic states is used in the partition function calculation. As a consequence, the results of classical Hopfield model can be recovered by the HFISG 2S model.

This work is organized in the following structure: Section 2 is devoted to derivation of thermodynamics and the order parameters. In Section 3, the phase diagrams temperature *versus* frustration level and temperature *versus* the chemical potential are presented. The entropy behavior *versus* temperature is also discussed. A special attention is given to the analysis of average number occupation *versus* chemical potential for high and low values of frustration level. Section 4 is held for conclusions.

2. Model

The model considered here is the HFISG model with a transverse magnetic field Γ. The Hamiltonian is given by

$$\hat{H} = -\sum_{ij} J_{ij}\hat{S}_i^z\hat{S}_j^z - 2\Gamma\sum_i \hat{S}_i^x, \tag{1}$$

where the summation over the indices ij runs over all combinations of pairs of sites of the lattice. In this model the interactions J_{ij} between spins are given as specified below:

$$J_{ij} = \frac{J}{2N}\sum_{\mu=1}^{p}\xi_i^\mu\xi_j^\mu, \tag{2}$$

where $\xi_i^\mu = \pm 1$, which follow the distribution $P(\xi_i) = \frac{1}{2}\delta_{\xi_i^\mu,+1} + \frac{1}{2}\delta_{\xi_i^\mu,-1}$. The spin operators in Eq. (1) are defined as Ref. [23], where $\hat{S}_i^z = \frac{1}{2}[\hat{n}_{i\uparrow} - \hat{n}_{i\downarrow}]$, $\hat{S}_i^x = \frac{1}{2}[c_{i\uparrow}^\dagger c_{i\downarrow} + c_{i\downarrow}^\dagger c_{i\uparrow}]$, $\hat{n}_{i\sigma} = c_{i\sigma}^\dagger c_{i\sigma}$ is the number operator, $c_{i\sigma}^\dagger$ ($c_{i\sigma}$) are fermion creation (destruction) operators, with $\sigma = \uparrow$ or $\downarrow$ indicating the spin projections.

The partition function is given in the Lagrangian path integral formalism where the spin operators are represented as anticommuting Grassmann fields (ϕ, ϕ^*). Thus, the partition function for 2S and 4S model can be represented in a compact form as

$$Z = \mathrm{e}^{\frac{s-2}{2}N\beta\mu}\int D(\phi^*\phi)\prod_j \frac{1}{2\pi}\int_0^{2\pi} dx_j\,\mathrm{e}^{-y_j}\mathrm{e}^{A_\Gamma + A_{\mathrm{SG}}} \tag{3}$$

with

$$A_\Gamma = \sum_j\sum_\omega \underline{\phi}_j^\dagger(\omega)\big[(i\omega + y_j)\underline{I} + \beta\Gamma\underline{\sigma}^x\big]\underline{\phi}_j(\omega), \tag{4}$$

where $\underline{\phi}_j^\dagger(\omega) = [\phi_{i\uparrow}^\dagger(\omega)\ \phi_{i\downarrow}^\dagger(\omega)]$, $\underline{I}$ is the unit matrix, $\underline{\sigma}^x$ is a Pauli matrix, $\beta = 1/T$ (T is the temperature), $y_j = ix_j$ for the 2S model or $y_j = \beta\mu$ for the 4S model, μ is the chemical potential, s is the state number per site allowed in each model,

$$A_{\mathrm{SG}} = \sum_{\Omega}\sum_{ij} \beta J_{ij} S_i^z(\omega') S_j^z(-\omega'), \tag{5}$$

and $S_i^z(\omega') = \frac{1}{2}\sum_\omega \sum_\sigma \sigma \phi_{i\sigma}^\dagger(\omega+\omega')\phi_{i\sigma}(\omega)$, where $\omega = (2m+1)\pi$ and $\omega' = 2m\pi$ ($m = 0, \pm 1, \ldots$) are the Matsubara's frequencies and $\sigma_s = +(-)$ if $\sigma = \uparrow(\downarrow)$. In this work, the problem is analyzed within SA which considers only the term when $\omega' = 0$ in Eq. (2) [18,23,24,26]. The grand canonical potential is obtained by using the replica method:

$$\beta\Omega = -\lim_{n\to 0} 1/(nN)\left(\left\langle\!\left\langle Z(n)\right\rangle\!\right\rangle_\xi - 1\right), \tag{6}$$

where $Z(n) \equiv Z^n$ and $\langle\!\langle \cdots \rangle\!\rangle_\xi$ means the configurational averaged over ξ. Thus, the replicated partition function can be presented as

$$Z(n) = \mathrm{e}^{\frac{s-2}{2}N\beta\mu} \int D(\phi_\alpha^*, \phi_\alpha) \prod_{i\alpha} \frac{1}{2\pi} \int_0^{2\pi} dx_{i\alpha}\, \mathrm{e}^{-y_{i\alpha}} \exp\left[A_\Gamma^\alpha + A_{\mathrm{SG}}^{stat,\alpha}\right], \tag{7}$$

where the action $A_{\mathrm{SG}}^{stat,\alpha}$ can be written as

$$A_{\mathrm{SG}}^{stat,\alpha} = \frac{\beta J}{2N} \sum_{\mu=1}^{p}\sum_{\alpha=1}^{n}\left(\sum_i \xi_i^\mu S_i^\alpha\right)^2 - \frac{\beta Jp}{2N}\sum_i\sum_{\alpha=1}^{n}(S_i^\alpha)^2 \tag{8}$$

when Eq. (2) is introduced in Eq. (5). In Eq. (8), α denotes the replica index and $S_i^\alpha \equiv S_i^\alpha(0)$.

The procedure to obtain $\langle\!\langle Z(n)\rangle\!\rangle_\xi$ within the one-step replica symmetry break (1S-RSB) approximation is shown in Appendix A. Introducing Eq. (21) in Eq. (6) and taking the limit $n \to 0$, the following expression for the grand canonical potential within 1S-RSB is obtained:

$$\beta\Omega = \frac{\beta^2 J^2 a R_0}{2} + \frac{\beta J m^2}{2} - \frac{1}{2}\frac{\beta J a q_0}{Q_1} + \frac{a}{2}\ln Q_0 + \frac{a}{2x}\ln\frac{Q_1}{Q_0} - \frac{s-2}{2}\beta\mu - \frac{1}{x}\int Dz \left\langle\!\!\left\langle \ln\int Dv\left(2K(z,v|\xi)\right)^x \right\rangle\!\!\right\rangle_\xi \tag{9}$$

where $a = p/N$ is the level of frustration, R_0, Q_0 and Q_1 are defined in Eq. (22) and

$$K(z,v|\xi) = \frac{s-2}{2}\cosh\beta\mu + \cosh\sqrt{\bar{\Delta}(z,v,w|\xi)}, \tag{10}$$

$\bar{\Delta}(z,v,w|\xi) = (\bar{H}(z,v,w|\xi))^2 + (\beta\Gamma)^2$ and $\bar{H}(z,v,w|\xi) = \beta J[\sqrt{ar_0}z + \sqrt{a(r_1-r_0)}v + \sqrt{a(\bar{r}-r_1-1/\beta J)}w + \xi m]$. The RS solution is recovered assuming $q_0 = q_1 = q$. The average over ξ in the grand canonical potential can be done using the parity properties of the functions dependent on z, v and w. The entropy can also be obtained directly from the grand canonical potential.

3. Numerical results

In this section, it is presented the numerical solutions for the coupled set of saddle point order parameters q_0, q_1, $\bar{q}$ and m in phase diagrams T/J vs a and T/J vs μ/J for several values of the level of frustration a and the transverse field Γ. The behavior of entropy S and the average of occupation number n are also presented. In the numerical results, it is assumed $J = 1$. For the paramagnetic (PM) phase, $q_1 = q_0 = m = 0$. The spin glass (SG) phase is obtained when $q_1 \neq q_0$ and $m = 0$. For $q_1 \neq 0$, $q_0 \neq 0$ and $m \neq 0$, the Mattis state (FE) is obtained. The HFISG model has been studied in two versions: the 2S and the 4S model as discussed previously.

Fig. 1 shows the phase diagrams T/J *versus* a for $\Gamma/J = 0$, $\Gamma/J = 0.5$ and $\Gamma/J = 0.75$ for 4S model at half-filling ($\mu/J = 0$). For $\Gamma = 0$, there are two distinct regions in the phase diagram. In the first one, for large level of frustration a, a second order PM/SG phase boundary T_{2f} appears when T/J decreases. While for small values of a, an additional first order SG/FE phase boundary T_{1f} arises when T/J decreases even more. When Γ is turned on, both T_{2f} and T_{1f} decrease. In particular, for $\Gamma/J = 0.75$, the FE phase is almost suppressed. The inset in Fig. 1 exhibits a comparison between the phase boundaries for the 2S model and the 4S model with $\mu = 0$ when $\Gamma = 0$. It shows that there is no qualitative difference between the phase boundaries obtained by 2S model and 4S model with $\mu = 0$. However, due to non-magnetic states, T_{2f} and T_{1f} in the 4S model are lower than that ones presented in the 2S model. Particularly, the phase diagram for the 2S model with $\Gamma = 0$ is similar to that one already found in the classical Hopfield model [20]. The effects of Γ over the phase boundaries found in Fig. 1 are consistent with those one obtained in Refs. [29,30].

In Fig. 2, the phase diagrams T/J *versus* μ/J are plotted for the level of frustration $a = 0.1$ and two values of Γ/J ($\Gamma/J = 0$ and $\Gamma/J = 0.75$). This value of a corresponds to the strong frustration scenario (see Fig. 1). In Fig. 2(a), the case $\Gamma = 0$ is displayed. This particular case has already been discussed in Ref. [11]. The main result is that below the tricritical point T_{tc} there are multiple SG solutions and the first order transition presents a reentrance that indicates an inverse transition. The presence of such transition is confirmed in the inset of Fig. 2(a), where the entropy S is plotted as a function of T/J. Nevertheless, when $\Gamma \neq 0$ the phase boundaries are deeply affected. For instance, in Fig. 2(b) ($\Gamma/J = 0.75$) the reentrance is completely destroyed even in the strong frustration limit. That can be seen in the inset of Fig. 2(b) where now the entropy of the SG phase is smaller than the PM phase.

Fig. 3 shows phase diagrams T/J *versus* μ/J for two values of Γ/J in a weak frustration scenario ($a = 0.0025$). In that case, the situation becomes more complex. There is now FE solutions for the order parameters and a triple point T_{tp} appears where the FE, SG and PM phases coexist. For $\Gamma = 0$ (see Fig. 3(a)), the reentrance is almost suppressed when compared to the $a = 0.1$ case. However, there is still a small range of chemical potential that presents reentrance and therefore an inverse freezing, as can be seen in the inset of Fig. 3(a).

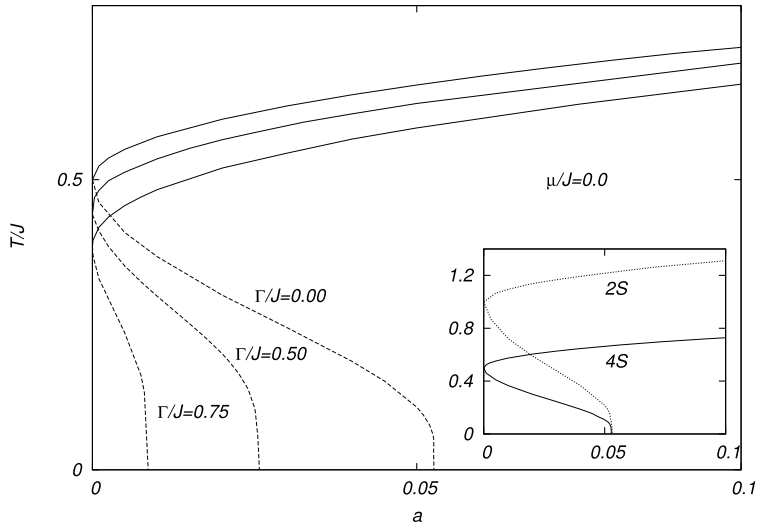

Fig. 1. Phase diagrams T/J *versus* a for $\mu/J = 0$ with $\Gamma/J = 0$, 0.5 and 0.75. Full lines indicate the second order transition between SG and PM phases $\mathbf{T}_{2f}$. Dashed lines indicate a first order transition $\mathbf{T}_{1f}$ between SG and FE phases. The inset shows a comparison between results obtained by 2S and 4S models.

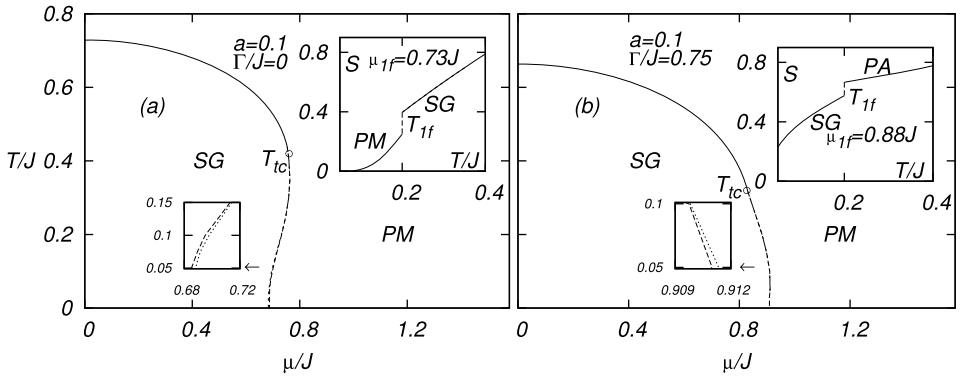

Fig. 2. Phase diagrams T/J *versus* μ/J for $a = 0.1$ with $\Gamma/J = 0$ and $\Gamma/J = 0.75$. T_{tc} indicates the tricritical point. The insets show the behavior of entropy S *versus* T/J for values of μ/J in the first order transition. In panels (a) and (b), a zoom indicates the difference between RS (dotted lines) and 1S-RSB (dashed lines) solutions.

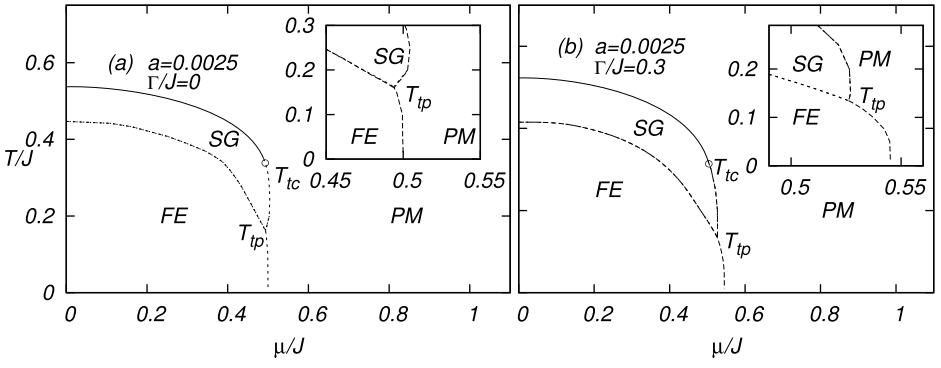

Fig. 3. Phase diagrams T/J *versus* μ/J for very low a ($a = 0.0025$) and two values of Γ/J: $\Gamma/J = 0.0$ for the left side panel and $\Gamma/J = 0.3$ for the right side panel. T_{tc} and T_{tp} indicate the tricritical point and triple point, respectively. The dashed lines indicate the first order transitions and the full lines indicate the second order transitions. The insets show the location of the triple points in details.

In Fig. 3(b), it is shown that the increase of Γ/J produces important effects on the phase boundaries. In particular, the reentrance between SG and PM phases is destroyed similarly to the situation shown in Fig. 2(b). Consequently, for $\Gamma/J = 0.3$, there is no more inverse freezing. It should be remarked that the phase boundary between FE and PM phases is also affected by the presence of Γ.

The average number occupation n as a function of μ/J is exhibited in Fig. 4 for several isotherms when $a = 0.1$. In Fig. 4(a), for the isotherm $T/J = 0.05$, the behaviour of n is given in two distinct situations (see Fig. 2), with and without inverse freezing which corresponds to $\Gamma = 0$ and $\Gamma/J = 0.75$, respectively. The result with $\Gamma = 0$ indicates that the double occupancy is dominant in the PM phase. While for $\Gamma = 0.75$, one has that n inside the SG phase tends to stay at half-filling until the phase transition occurs, even with the increase of μ. In this sense, the presence of Γ seems to redistribute charges in the SG phase in a way that the contribution of non-

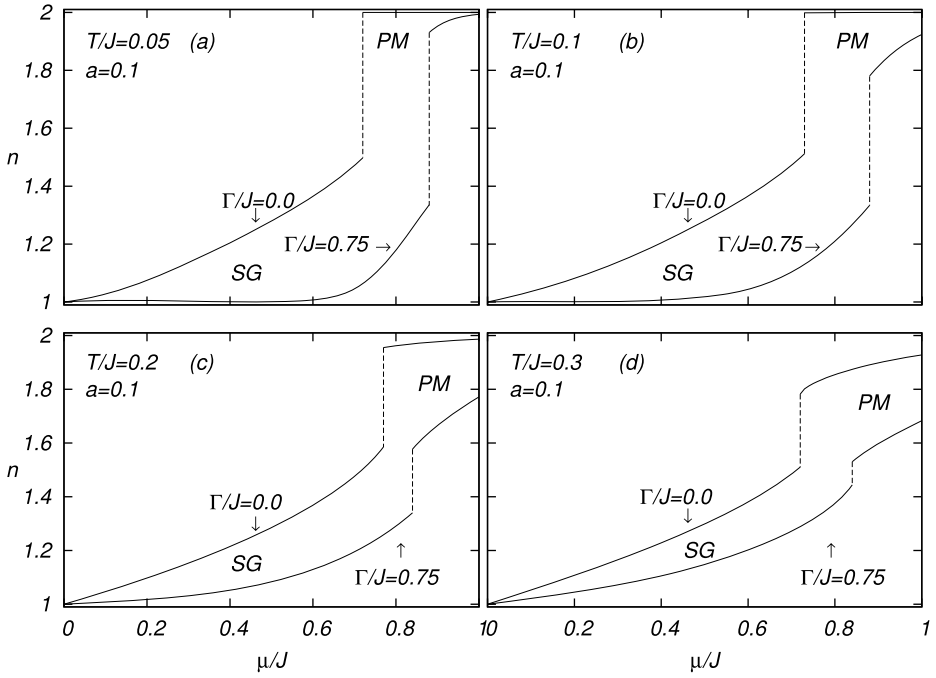

Fig. 4. Average of occupation number n *versus* μ/J for $a = 0.1$ and values of T/J in the first order transition region with two values of Γ ($\Gamma/J = 0$ and $\Gamma/J = 0.75$). The vertical lines indicate the first order transition between the SG and the PM phases.

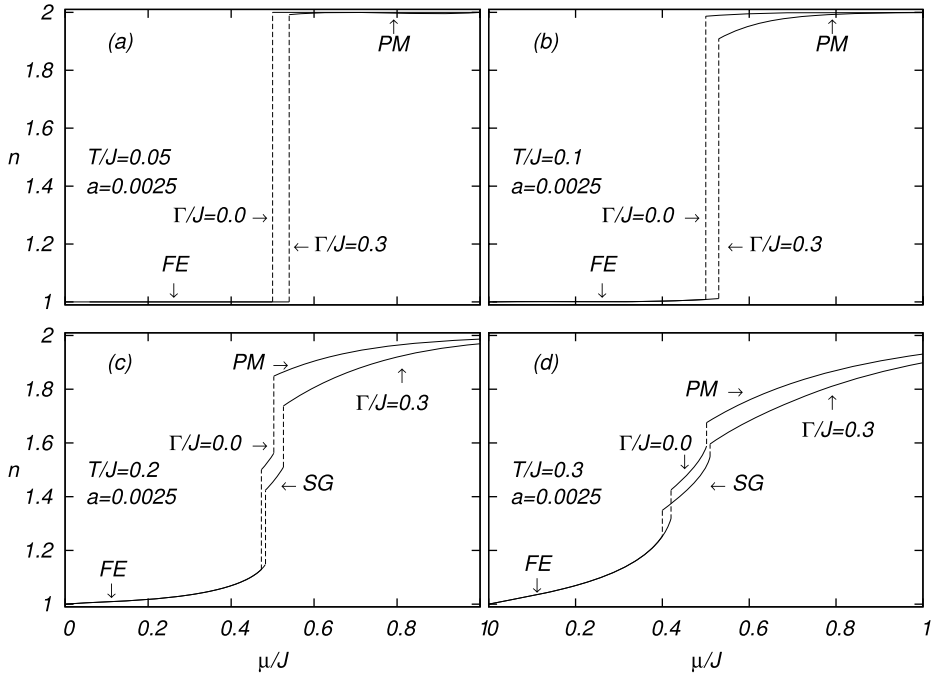

Fig. 5. Behavior of occupation number n *versus* μ/J for $a = 0.0025$, two values of Γ/J (0 and 0.3) and several temperatures: $T/J = 0.05$, 0.1, 0.2 and 0.3 for the panels (a), (b), (c) and (d), respectively. In panels (a) and (b), the vertical lines indicate the FE/PM first order transitions. In panels (c) and (d), the left and the right vertical lines indicate the FE/SG and the SG/PM first order transitions, respectively.

magnetic states is unfavored as compared with the $\Gamma = 0$ situation, particularly at low temperatures. In Figs. 4(b)–4(d), it is shown that the enhancement of the temperature gradually modifies the initial behaviour of n shown in Fig. 4(a). The behaviour of n for $\Gamma = 0$ and $\Gamma/J = 0.75$ becomes increasingly similar. For instance, in Fig. 4(d), for $T/J = 0.3$, it can be seen that the dominance of double occupation in the PM phase disappears in the case $\Gamma = 0$. With respect to the SG phase, the field $\Gamma/J = 0.75$ is no longer able to keep n at the half-filling occupation when μ increases. It should be remarked, that in this particular isotherm there is no more inverse freezing (see Fig. 2).

Fig. 5 illustrates the behavior of n for small level of frustration ($a = 0.0025$) with $\Gamma = 0$ and $\Gamma/J = 0.3$ also for several isotherms. For $T/J = 0.05$, the results are shown in Fig. 5(a). For this isotherm there is only a FE/PM phase transition with no inverse melting (see Fig. 3). In that case when μ increases, the average occupation remains with $n = 1$ in the SG phase and then with $n = 2$ in the

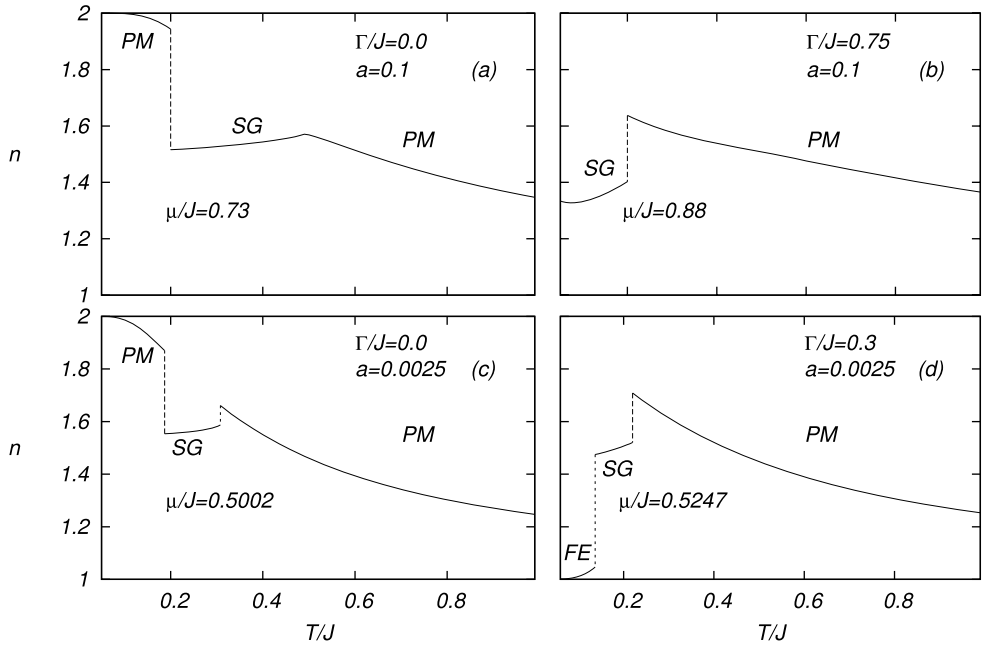

Fig. 6. Average of occupation number n as a function of T/J for values of μ in the first order transition region where: (a) $a = 0.1$, $\mu/J = 0.73$ and $\Gamma/J = 0.0$; (b) $a = 0.1$, $\mu/J = 0.88$ and $\Gamma/J = 0.75$; (c) $a = 0.0025$, $\mu/J = 0.5002$ and $\Gamma/J = 0.0$; (d) $a = 0.0025$, $\mu/J = 0.5247$ and $\Gamma/J = 0.3$.

PM one. The presence of Γ in this case only displaces the location of the first order boundary transition for a larger value of μ. In the remaining Fig. 5(b)–(d), the effects of the temperature start to become important. In Fig. 5(c)–(d) with isotherms $T/J = 0.2$ and $T/J = 0.3$, respectively, there is first a FE/SG phase transition and then a SG/PM one with inverse freezing when $\Gamma = 0$. In that case, when Γ is turned on, n remains unaffected in the FE phase while in the SG and PM phases n is basically that one discussed previously in Fig. 4.

Fig. 6 shows n *versus* T/J for $a = 0.1$ with $\Gamma = 0.0$, and 0.75 and $a = 0.0025$ with $\Gamma = 0.0$ and $0.3J$. The values of μ are chosen in order to cross the first order phase transitions when the temperature is decreased and, in particular, the inverse freezing when $\Gamma = 0$ (see Figs. 2 and 3). In the strong frustration scenario ($a = 0.1$), Fig. 6(a) shows the behaviour of n for $\mu/J = 0.73$ and $\Gamma = 0$ when the temperature is changed. In that case, there is firstly, a second order phase transition PM/SG and then, the inverse freezing SG/PM (see Fig. 2(a)). The aspect that should be remarked is that the behaviour of n at higher and lower temperature in the PM phase is clearly distinct. The PM phase at lower T/J (which is involved in an inverse freezing) presents n closer to the double occupation as compared to the PM phase at high T/J. This result indicates a difference in the nature of PM phase at lower temperature as compared to that one found at higher temperature. Fig. 6(b) corresponds to $\mu/J = 0.88$, but now with $\Gamma/J = 0.75$ (see Fig. 2(b)). This figure shows that n in the SG phases decreases after the first order phase transition PM/SG. In the weak frustration scenario ($a = 0.0025$) for $\mu/J = 0.50$ and $\Gamma = 0$, Fig. 6(c) shows qualitative the same behavior found in Fig. 6(a). Particularly concerning the behaviour of n in the PM phase for higher and lower temperature (also involved in an inverse freezing). In Fig. 6(d) for $\mu/J = 0.5247$ and $\Gamma/J = 0.3$ (see Fig. 3(b)), the PM phase at lower temperature is replaced by the FM one which has n quite close to the half-filling.

4. Conclusions

The present work studied the HFISG model with a transverse magnetic field Γ. The model has been presented in two versions: 2S model and 4S model. In both versions, the mean field calculations have been performed using static approximation and 1S-RSB scheme. Particularly, the inverse freezing in the 4S model has been studied in the grand canonical ensemble for several frustration regimes and values of Γ.

Our results indicate that spin flip mechanism provided by the transverse field Γ suppresses the inverse freezing. Mostly important is that the suppression occurs for any value of the level of frustration a. In the strong frustration scenario, where the reentrance of the first order boundary phase SG/PM is more pronounced, it is needed a larger value of Γ as compared to the weak frustration one. However, besides this adjustment in its strength, the Γ field produces the same effect which leads to the ending of the inverse freezing. We remark that the result in the strong frustration scenario is in agreement with the fermionic SK-type model (the so-called FISG model) for the SG problem studied in Ref. [10].

The effect of Γ which can explain the ending of the inverse freezing in the present work appears clearly in the behaviour of average of occupation number n. In the case of the strong frustration scenario this effect is, at lower temperature, to maintain $n = 1$ even when μ increases. In that sense, Γ would act to eliminate the non-magnetic states. Thus one can conclude that the increase of Γ can suppress the inverse freezing by redistributing charge in a such way that destroys the dilution in the problem. That indicates dilution as a necessary condition to produce naturally inverse transition. It should be remarked that the decrease of n due to changes in Γ does not ensure that the non-magnetic states in the sites are avoided. However, results found in the FISG model [23] indicate that the non-magnetic states in the sites become increasingly not relevant for higher values of Γ and lower values of temperature. One could assume that the same process is present in the HFISG model.

Nevertheless, the dilution is not enough to explain the natural existence of inverse freezing in the HFISG model. For instance, in the strong frustration regime and $\Gamma = 0$ when there is inverse freezing, albeit the PM phase at lower temperature is more diluted than the SG

one, this last phase still presents larger entropy. Therefore, our results clearly suggest that the key element to rise naturally inverse freezing in the HFISG model is the combined effect of dilution and frustration. One could put in more general terms the previous assumption. The natural emergence of inverse freezing in a magnetic model would appear since there is a mechanism favoring non-interacting states at lower temperature (as the anisotropy in the GS model) necessarily combined to a degeneracy of the interacting state given by frustration. We are currently investigating others magnetic models which present the mentioned combination.

Appendix A. The procedure to obtain $\langle\langle Z(n)\rangle\rangle_\xi$

In this appendix, the procedure to obtain $\langle\langle Z(n)\rangle\rangle_\xi$ within the one-step replica symmetry breaking (1S-RSB) ansatz is presented. The introduction of the order parameters in Eq. (7) follows closely to Ref. [11]. As a result, the following expression for $\langle\langle Z^n\rangle\rangle_\xi$ is obtained:

$$\left\langle\!\left\langle Z^n\right\rangle\!\right\rangle_\xi = \int \prod_\alpha Dm_\alpha^1 \int \prod_{\alpha\beta} \frac{dr'_{\alpha\beta}\, dq_{\alpha\beta}}{2\pi} \mathrm{e}^{-\beta N \langle\langle \Phi(q_{\alpha\beta}, r'_{\alpha\beta}, m_\alpha^1)\rangle\rangle_\xi} \tag{11}$$

with

$$\left\langle\!\left\langle \Phi\left(q_{\alpha\beta}, r'_{\alpha\beta}, m_\alpha^1\right)\right\rangle\!\right\rangle_\xi = \frac{J}{2}\sum_\alpha \left(m_\alpha^1\right)^2 - \frac{i}{\beta N}\sum_{\alpha\beta} r'_{\alpha\beta} q_{\alpha\beta} + \frac{1}{2\beta N}(p-s)Tr\ln\Lambda - \frac{1}{\beta}\ln\left\langle\!\left\langle \Theta\left(r'_{\alpha\beta}, m_\alpha^1, \xi\right)\right\rangle\!\right\rangle_\xi, \tag{12}$$

$\Lambda_{\alpha\beta} = \delta_{\alpha\beta} - \beta J q_{\alpha\beta}$ and

$$\Theta\left(r'_{\alpha\beta}, m_\alpha^1, \xi\right) = \prod_\alpha \mathrm{e}^{(\frac{s-2}{2})\beta\mu_\alpha} \frac{1}{2\pi}\int_0^{2\pi} dx_\alpha\, \mathrm{e}^{-y_\alpha} \int D\left(\phi_\alpha^*\phi_\alpha\right) \mathrm{e}^{-\frac{i}{N}\sum_{\alpha\beta} r'_{\alpha\beta} S^\alpha S^\beta - \frac{\beta J}{2N} p \sum_\alpha (S^\alpha)^2} \mathrm{e}^{\beta J \sum_\alpha m_\alpha^1 (\xi^1 S^\alpha) + \sum_\alpha A_\Gamma^\alpha} \tag{13}$$

with

$$A_\Gamma^\alpha = \sum_\omega \underline{\phi}_\alpha^\dagger(\omega)\left[(i\omega + y)\underline{I} + \beta\Gamma\underline{\sigma}^x\right]\underline{\phi}_\alpha(\omega) \tag{14}$$

where $\underline{I}$ is the unit matrix, $\underline{\sigma}^x$ is a Pauli matrix and the order parameters m_α^1, $r'_{\alpha\beta}$ and $q_{\alpha\beta}$ have been introduced to linearize the quadratic terms in $\langle\langle Z^n\rangle\rangle_\xi$. The integrals over these order parameters are evaluated by the steepest descent method in the thermodynamic limit $N\to\infty$, which results in

$$m_\alpha^1 = \left\langle\!\left\langle \frac{1}{N}\sum_i \xi_i^1 \langle S_i^\alpha\rangle \right\rangle\!\right\rangle_\xi, \qquad q_{\alpha\beta} = \left\langle\!\left\langle \frac{1}{N}\sum_i \langle S_i^\alpha S_i^\beta\rangle \right\rangle\!\right\rangle_\xi, \qquad -ir'_{\alpha\beta} = \frac{(\beta J)^2 Np}{2}\left\langle\!\left\langle \frac{1}{p}\sum_{\varrho=2}^{p} m_\alpha^\varrho m_\beta^\varrho \right\rangle\!\right\rangle_\xi = \frac{(\beta J)^2}{2} p r_{\alpha\beta} \tag{15}$$

where $m_\alpha^\varrho = \sum_i \xi_i^\varrho \langle S_i^\alpha\rangle/N$ for $\varrho \geqslant 2$.

In the 1S-RSB solution, the order parameters $q_{\alpha\beta}$ and $r_{\alpha\beta}$ are parametrized as:

$$q_{\alpha\beta} = \begin{cases} \bar{q} & \text{se } \alpha = \beta, \\ q_1 & \text{se } I(\alpha/x) = I(\beta/x), \\ q_0 & \text{se } I(\alpha/x) \neq I(\beta/x), \end{cases} \qquad r_{\alpha\beta} = \begin{cases} \bar{r} & \text{se } \alpha = \beta, \\ r_1 & \text{se } I(\alpha/x) = I(\beta/x), \\ r_0 & \text{se } I(\alpha/x) \neq I(\beta/x) \end{cases} \tag{16}$$

and order parameters m_α^1 are invariant with respect to permutations of replicas: $m_\alpha^1 = m$, where $\alpha = 1, \ldots, n$. Particularly, Eq. (13) in the 1S-RSB scheme becomes

$$\begin{aligned}&\Theta\left(\{r\}, m, \xi\right)\\ &= \prod_\alpha \int_0^{2\pi} Dx_\alpha \int D\left(\phi_\alpha^*\phi_\alpha\right) \mathrm{e}^{\frac{\beta^2 J^2 a}{2}\left[(\bar{r} - r_1 - 1/\beta J)\sum_{\alpha=1}^n (S^\alpha)^2 + (r_1 - r_0)\sum_{l=1}^{n/x}\left(\sum_{\alpha=(l-1)x+1}^{lx} S^\alpha\right)^2 + r_0\left(\sum_{\alpha=1}^n S^\alpha\right)^2\right] + \beta J\sum_{\alpha=1}^n (\xi m S^\alpha) + \sum_\alpha A_\Gamma^\alpha}\end{aligned} \tag{17}$$

where $Dx_\alpha = \mathrm{e}^{(\frac{s-2}{2})\beta\mu_\alpha}\frac{1}{2\pi} dx_\alpha\, \mathrm{e}^{-y_\alpha}$ and $a = p/N$ is the level of frustration. The quadratic forms into the functional $\Theta(\{r\}, m, \xi)$ can be linearized by Hubbard–Stratonovich transformations where new auxiliary fields are introduced in the problem. Therefore, one has:

$$\Theta\left(\{r\}, m, \xi\right) = \int Dz \left[\int Dv \left(\int_0^{2\pi} Dx \int Dw \int D\left(\phi^*\phi\right) \exp\sum_\omega \underline{\phi}^*(\omega) G^{-1}(\omega)\underline{\phi}(\omega)\right)^x\right]^{n/x}, \tag{18}$$

with $\underline{\phi}^*(\omega) = [\phi_{i\uparrow}^*(\omega)\ \phi_{i\downarrow}^*(\omega)]$, $Dy = \frac{dy\,\mathrm{e}^{-\frac{y^2}{2}}}{\sqrt{2\pi}}$ $(y = z, v, w)$,

$$G^{-1}(\omega) = (i\omega + y)\underline{I} + \beta\Gamma\underline{\sigma}^x + \left[\bar{h}(z, v, w) + \beta J(\xi m)\right]\underline{\sigma}^z \tag{19}$$

where $\underline{\sigma}^z$ is a Pauli matrix. The local spin glass component of the random field $\bar{h}(z, v, w)$ is defined by

$$\bar{h}(z, v, w) = \beta J\left[\sqrt{ar_0}z + \sqrt{a(r_1 - r_0)}v + \sqrt{a(\bar{r} - r_1 - 1/\beta J)}w\right]. \tag{20}$$

The functional integral over the Grassmann variables, as well as the sum over the Matsubara's frequencies in Eq. (18), can be performed following closely the procedure given in Refs. [23,31]. As a result, the following equation for $\langle\langle Z^n\rangle\rangle_\xi$ can be obtained

$$\langle\langle Z^n\rangle\rangle_\xi = 1 - nN\left[\frac{\beta^2 J^2 a}{2}[R_0 + n r_0 q_0] + \frac{\beta J m^2}{2} - \frac{a}{2n}\ln\left[1 - \frac{n\beta J q_0}{Q_1}\right] + \frac{a}{2}\ln Q_0 + \frac{a}{2x}\ln\frac{Q_1}{Q_0} - \frac{s-2}{2}\beta\mu - \frac{1}{x}\int Dz\left\langle\left\langle \ln\int Dv\big(2K(z,v|\xi)\big)^x\right\rangle\right\rangle_\xi\right] \tag{21}$$

where

$$R_0 = \bar{r}\bar{q} - (1-x)r_1 q_1 - x r_0 q_0, \qquad Q_1 = 1 - \beta J\big[\bar{q} - q_1 + x(q_1 - q_0)\big], \qquad Q_0 = 1 - \beta J(\bar{q} - q_1) \tag{22}$$

and $K(z, v|\xi)$ is defined in Eq. (10).

Appendix B. Order parameters

The set of equations for the order parameters m, q_0, q_1, $\bar{q}$ and the block size parameter x in the 1S-RSB approximation can be found from Eq. (9) using the saddle point conditions, which result in

$$m = \int Dz\left\langle\left\langle \frac{\int Dv K(z,v|\xi)^{x-1}\xi\int Dw\bar{h}(z,v,w|\xi)\sinh\sqrt{\bar{\Delta}(z,v,w|\xi)}}{\int Dv K(z,v|\xi)^x\sqrt{\bar{\Delta}(z,v,w|\xi)}}\right\rangle\right\rangle_\xi, \tag{23}$$

$$q_0 = \int Dz\left\langle\left\langle \left(\frac{\int Dv K(z,v|\xi)^{x-1}\int Dw\bar{h}(z,v,w|\xi)\sinh\sqrt{\bar{\Delta}(z,v,w|\xi)}}{\int Dv K(z,v|\xi)^x\sqrt{\bar{\Delta}(z,v,w|\xi)}}\right)^2\right\rangle\right\rangle_\xi, \tag{24}$$

$$q_1 = \int Dz\left\langle\left\langle \frac{\int Dv K(z,v|\xi)^{x-2}[\int Dw\bar{h}(z,v,w|\xi)\sinh\sqrt{\bar{\Delta}(z,v,w|\xi)}]^2}{\int Dv K(z,v|\xi)^x\bar{\Delta}(z,v,w|\xi)}\right\rangle\right\rangle_\xi, \tag{25}$$

$$\bar{q} = \int Dz\left\langle\left\langle \frac{\int Dv K(z,v|\xi)^{x-1}\int Dw[\frac{h^2(z,v,w|\xi)\cosh\sqrt{\bar{\Delta}(z,v,w,\xi)}}{\bar{\Delta}(z,v,w|\xi)} + \frac{(\beta\Gamma)^2\sinh\sqrt{\bar{\Delta}(z,v,w|\xi)}}{\bar{\Delta}(z,v,w|\xi)^{3/2}}]}{\int Dv K(z,v|\xi)^x}\right\rangle\right\rangle_\xi, \tag{26}$$

with the equation for the x parameter given as

$$\frac{1}{x}\int Dz\left\langle\left\langle \ln\int Dv K(z,v|\xi)^x\right\rangle\right\rangle_\xi - \frac{1}{x}\int Dz\left\langle\left\langle \frac{\int Dv K(z,v|\xi)^x\ln K(z,v|\xi)^x}{\int Dv K(z,v|\xi)^x}\right\rangle\right\rangle_\xi + \frac{\beta J a}{2}\left(\frac{q_0}{Q_1} - \frac{q_1}{Q_0}\right) - \frac{a}{2x}\ln\frac{Q_1}{Q_0} = 0. \tag{27}$$

The elements of matrix r are given by

$$r_0 = \frac{q_0}{Q_1^2}, \qquad r_1 - r_0 = \frac{q_1 - q_0}{Q_0 Q_1}, \qquad \bar{r} - r_1 = \frac{1}{Q_0}. \tag{28}$$

References

[1] A.L. Greer, Nature (London) 404 (2000) 134.
[2] S. Rastogi, G.W.H. Höhne, A. Keller, Macromolecules 32 (1999) 8897;
N.J.L. van Ruth, S. Rastogi, Macromolecules 37 (2004) 8191.
[3] O. Portmann, A. Vaterlaus, D. Pescia, Nature (London) 422 (2001) 701.
[4] N. Avraham, B. Khaykovich, Y. Myasoedev, M. Rapoport, H. Shtrikman, D.E. Feldman, T. Tamegai, P.H. Kes, M. Li, M. Konczykowski, K. van der Beek, E. Zeldov, Nature (London) 411 (2001) 451.
[5] N. Schupper, N.M. Shnerb, Phys. Rev. Lett. 93 (2004) 037202;
N. Schupper, N.M. Shnerb, Phys. Rev. E 72 (2005) 046107.
[6] A. Crisanti, L. Leuzzi, Phys. Rev. Lett. 95 (2005) 087201.
[7] M.R. Feeney, P.G. Debenedetti, F.H. Stillinger, J. Chem. Phys. 119 (2003) 4582.
[8] M. Sellito, Phys. Rev. B 73 (2006) 180202(R).
[9] S. Prestipino, Phys. Rev. E 75 (2007) 011107.
[10] S.G. Magalhaes, C.V. Morais, F.M. Zimmer, Phys. Rev. B 77 (2008) 134422.
[11] S.G. Magalhaes, C.V. Morais, F.M. Zimmer, Phys. Rev. B 81 (2010) 014207.
[12] M. Paoluzzi, L. Leuzzi, A. Crisanti, Phys. Rev. Lett. 104 (2010) 120602.
[13] F.A. da Costa, Phys. Rev. B 82 (2010) 052401.
[14] A. Scholl, L. Kilian, Y. Zou, J. Ziroff, S. Hame, F. Reinert, E. Umbach, R.H. Fink, Science 329 (2010) 303.
[15] M. Blume, Phys. Rev. 141 (1996) 517;
H.W. Capel, Physica (Amsterdam) 32 (1966) 966.
[16] S.K. Ghatak, D. Sherrington, J. Phys. C 10 (1977) 3149.
[17] E. Fradkin, B.A. Huberman, S.H. Shenker, Phys. Rev. B 18 (1978) 4789.
[18] A. Theumann, M.V. Gusmão, Phys. Lett. A 105 (1984) 311.
[19] R. Oppermann, A. Muller-Groeling, Nucl. Phys. B 401 (1993) 507.
[20] D.J. Amit, Modellin Brain Function, The World of Attractor Neural Networks, Cambridge University Press, Cambridge, England, 1989.
[21] D. Sherrington, S. Kirkpatrick, Phys. Rev. B 17 (1978) 4384.
[22] J.P. Provost, G. Valee, Phys. Rev. Lett. 50 (1983) 598.
[23] A. Theumann, A.A. Schmidt, S.G. Magalhaes, Physica A 311 (2002) 498.
[24] F.M. Zimmer, S.G. Magalhães, Physica A 359 (2006) 380.

[25] S.G. Magalhaes, F.M. Zimmer, C.V. Morais, Physica A 388 (2009) 2140.
[26] A.J. Bray, M.A. Moore, J. Phys. C: Sol. State 13 (1980) L655.
[27] G. Parisi, J. Phys. A: Math. Gen. 13 (1980) 1101.
[28] F. da Costa, C.S.O. Yokoi, S.R.A. Salinas, J. Phys. A 27 (1994) 3365.
[29] Y.Q. Ma, Y.M. Zhang, Y.G. Ma, C. de Gong, Phys. Rev. E 47 (1993) 3985.
[30] H. Nishimori, Y. Nonomura, J. Phys. Soc. Japan 65 (1996) 3780.
[31] F.M. Zimmer, S.G. Magalhaes, Phys. Rev. B 74 (2006) 012202.